

# Multifractal analysis of turbulent wakes for model wind turbines using large eddy simulation

J. Tellez-Alvarez\*, A. Kryuchkova\*\*, S. Strijhak\*\* and J.M. Redondo\*\*\*  
Corresponding author: jackson.david.tellez@upc.edu

\* Research Group FLUMEN, Technical University of Catalonia (UPC) Barcelona, Spain.

\*\* Ivannikov Institute for System Programming of the Russian Academy of Science (ISP RAS), Moscow, Russia.

\*\*\* Dept. Física, Barcelona Tech. Campus Nord (UPC). Barcelona, Spain.

**Abstract:** Over the last years it has become evident that one of the greatest problems during wind turbine operations is related to intermittency between turbulent flow and the blades. An adjacent problem consists in coupling and wake effects of one turbine on its neighbor on extended sites. This research has focused on the detailed study of wind wakes behavior and energy analysis using experiments and fluid simulations of high resolution in both physical and Fourier spaces. Analogously to compressibility and shock interactions rotation and stratification can produce resonant interactions between turbines and lead to damage effects. In this paper numerical results of Large Eddy Simulation in OpenFOAM SOWFA library are presented. Furthermore, scaling of the wake turbulence and wakes interaction with the Neutral Atmospheric Boundary Layer is undertaken via multifractal analysis. Several turbulent indicators, topological aspects and intermittency between a single, two and twelve wind turbines were compared. The study has shown a non-linear growth of intermittency at large scales when several wakes interact with each other. Supplementary findings on spectra and multifractal indicators seem to be extremely useful to optimize wind farms functioning and to increase their performance.

*Keywords:* Wind energy, fractal dimension, numerical simulation, Large Eddy Simulation (LES), Complex Turbulence, Compressibility.

## 1. Introduction

Wind energy is an important part of renewable energy sources. At present it has found a range of widespread applications but the scientific community is still aware of the destructive power of wind resonances and intermittency. The most recent tendencies suppose studying of detailed dynamics of turbulent wakes produced by wind turbines and their performance in wind farms [1]. Large-eddy simulation (LES) has recently been well applied in the context of wind turbines over flat and complex terrains. An open-source library SOWFA as part of OpenFOAM which includes several incompressible solvers and utilities was used [2]. The mathematical model had the equations for mass, momentum and energy conservation for incompressible flow. Large-scale vortex structures were

simulated by means of filtered equations integration. Small eddies, for which the size didn't exceed a size of grid cell, were modelled by means of a Lagrangian-averaged scale-independent dynamic Smagorinsky model. ABL Solver is used for studying physical processes in Neutral Atmospheric Boundary Layer (ABL). One of the specific solvers called `pisoFoamTurbine` implementing Actuator Lines Model to represent wind turbine functioning was used. Next we describe the model used and in section 3 we present the way in which intermittency is related to fractality of the wakes. Further we compile characteristics of wakes produced by 1, 2, 4 and 12 turbines to assess their interactions. Finally, ground and Atmospheric Boundary Layer effects are investigated and a discussion on multi-fractality of the wakes is given in conclusion.

## 2. Mathematical model of Large Eddy Simulation

The mathematical model includes mass and momentum conservation laws for incompressible flow for implemented in `pisoFoamTurbine` solver. Large-scale vortex structures are accounted for by means of filtered equations integration [3]. A box filter was used to obtain the filtered equations. Small eddies, for which the size didn't exceed a size of grid cell, were modelled by means of a Lagrangian-averaged scale-independent (LASI) dynamic Smagorinsky model [4].

$$\frac{\partial \bar{u}_j}{\partial x_j} = 0 \quad (1)$$

where  $\bar{u}_j = u_j - u'_j$  - vector of value for resolved-scale velocity after the procedure of a filtration the equations.

$$\frac{\partial \bar{u}_i}{\partial t} + \frac{\partial}{\partial x_j} (\bar{u}_j \bar{u}_i) = -2\varepsilon_{ijk} \Omega_j \bar{u}_k - \frac{\partial \tilde{p}}{\partial x_i} - \frac{\partial}{\partial x_j} (R_{ij}^D) + \left( \frac{\rho_b}{\rho_0} - 1 \right) g_i - \left\langle \frac{\partial p}{\partial x_i} \right\rangle + f_i \quad (2)$$

where  $\varepsilon_{ijk}$  - alternating unit tensor,  $\Omega_j$  - planetary rotation rate vector at the point of interest on the

planet,  $\tilde{p}$  - pressure,  $R_{ij}^D$  - so-called deviatoric part of the sub-grid-scale (SGS) stress tensor,  $\frac{\rho_b}{\rho_0}$  -

buoyancy force term,  $g_i$  - vertical gravitation vector,  $\frac{\partial p}{\partial x_i}$  - pressure gradient in horizontal direction.

The mathematical model was realized in SOWFA (Simulator for On/Offshore Wind Farm Application) code. SOWFA is an OpenFOAM based incompressible atmospheric/wind farm Large-Eddy Simulation (LES) library based on finite-volume method. It allows to model wind turbines either with actuator lines or actuator disk models [5, 6].

Considering the characteristic sizes of wind turbine blades, Re numbers can reach an order of  $Re=10e7-10e8$ . It is difficult to resolve all flow scales by means of LES since too big numerical grids would be required for this purpose. It is well-known that Actuator Line Model (ALM) approach doesn't demand too detailed grids around the turbine blades. This approach allows to represent various types of vortexes, viz wake, trailer, root and boundaries vortexes. In scope of ALM turbine blades are approximated by separate flat sections with given profile, chord and twist. Values of lift and drag forces are collected in tables for each profile. The force projected on the flow is equal to the aero dynamical force applied on operating turbine blades. Procedure of force projection comes to a number of separate terms adding in the momentum equation. The resultant force  $F$  is determined with following technique [5, 6]:

$$f_i^{turbine}(r) = \frac{F_i^{actuator}}{\epsilon ps^3 \pi^{3/2}} \exp\left[-\left(\frac{r}{\epsilon ps}\right)^2\right], \quad (3)$$

where  $F_i^{actuator}$  is actuator point force, projected as a body force onto Computational Fluid Dynamics (CFD) grid,  $r$ - distance between CFD cell center and actuator point,  $\epsilon ps$  is of Gaussian filter width related to the initial intermittency. Further details can be found in [15].

### 3. Turbulence, Intermittency and Fractal Dimensions

One of the ways to statistic behavior of turbulent wakes is based on using of structure function proposed originally in theory of Kolmogorov (K41). The theory has an ability to get more robust statistics; it helps to identify coherent flow structures and also to determine isotropy levels by a statistical description pooled in PDF or spectrally. Longitudinal structure function  $B(R)$  of order  $P$  is defined in terms of the moments of the velocity increments:

$$B(R)^P = \left\langle \left( u(x+R) - u(x) \right)^P \right\rangle = \left\langle \delta_R(u)^P \right\rangle, \quad (4)$$

where  $u$  is streamwise (or spanwise with reference to Transverse Structure functions) velocity component at location  $x$ ,  $R$  is spatial separation distance between two points which quantifies indeed a particular scale of interest.

Kolmogorov (K41) introduced a similarity theory for homogenous and isotropic turbulent flows which states that the mean dissipation energy  $\epsilon$  is scale-invariant and the structure function is then given by:

$$B(R)^P \sim \langle \epsilon \rangle^{P/3} R^{P/3} \quad (5)$$

Higher order statistics displays discrepancies while comparing the evaluation as proposed by K41 to experimental data where intermittency is taken into account and a significant deviation from the mean flow is found in the dissipation.

Kolmogorov (K62) refined the previous similarity theory and presented a log-normal distribution for scale dependence within the dissipation range as:

$$B(R)^P \sim \langle \epsilon_R \rangle^{P/3} R^{P/3} \sim R^{\xi_p} \quad (6)$$

The intermittency phenomenon can be accounted for via the scaling exponent of appropriate moments which associates the separation scales between two neighboring points [7,8].

$$\xi_p = \frac{p}{3} + \frac{1}{18} \mu p (3-p) \quad (7)$$

where  $\mu$  - intermittency exponent which characterizes the intermittency of the energy dissipation fluctuation;  $\xi_p$  - scaling exponent.

Frisch introduced Beta-model, which is dependent on the energy cascade and concentrates on the nonlinearity transmission along inertial subrange [9]. Scaling exponent of the Beta model can be expressed as:

$$\xi_p = \frac{p}{3} + \frac{1}{3} (3-H)(3-p) \quad (8)$$

where  $H$  - the Hausdorff dimension, also related to the Hurst Exponent (Hu) or the Holden (Ho) indicator (see [14], [15]) otherwise known as self-similarity dimension of dissipative structures and defined in certain 3D cases as co-dimension 3-D ( $H=3-\mu$ ).

Intermittency in turbulence has been investigated for different types of flows such as free jet [10], Atmospheric Boundary Layer flow [11], free jet and cylinder [12], wake flow for fractal grid [13], wake flow in experiment for 3x3 wind turbine array [14].

The relationship between intermittency, energy and the maximum fractal dimension is given by:

$$E_l \approx v_l^2 p_l = v_l^2 \left( \frac{l}{l_0} \right)^{3-D} \quad (9)$$

The flow of energy  $\Pi$  from scales  $l$  to smaller scales is equal to  $E_l/t_l$ . so that,

$$\Pi_l \approx \frac{v_l^3}{l} \left( \frac{l}{l_0} \right)^{3-D} \quad (10)$$

We usually assume that for high Reynolds numbers there is an inertial range in which the energy flow is independent from  $l$ :

$$\Pi_l \approx \varepsilon \approx \frac{v_0^3}{l_0} \quad (11)$$

An implication of the previous expression in case when we recover the initial scale  $l_0$  is as follows:

$$v_l \approx v_0 \left( \frac{l}{l_0} \right)^{\frac{1}{3} + \frac{3-D}{3}} \quad (12)$$

and

$$t_l \approx \frac{l}{v_l} \approx \frac{l_0}{v_0} \left( \frac{l}{l_0} \right)^{\frac{2}{3} + \frac{3-D}{3}} \quad (13)$$

The above equation can be seen as the statement that the velocity field has the scalar exponent

$$h = \frac{1}{3} - \frac{3-D}{3} \quad (14)$$

In the series  $\zeta$  of fractal dimension  $D$ , in which the waterfall accumulates. This new formulation will be useful for the generalization to multifractals.

We now turn to the structure functions. At phenomenological level it is difficult to distinguish functions of longitudinal structure and those related to the other components. On this stage we must avoid such a distinctions and simply indicate the function of the structure of order  $p$  of  $\langle \delta v_p^l \rangle$ .

There are two contributions to this quantity. Firstly, there is a factor originating from the most active eddies due to forcing intermittency. Secondly, there is an additional intermittency factor  $p_l = (l/l_0)^{3-D}$  that gives us volume fraction of active swirls of scale  $l$ . This factor is geometrically driven by the fractal nature of the non-homogeneous dissipation distribution which was widely considered in (K62). By the aid of the previous expression, we obtain:

$$S_p(l) = \langle \delta v_l^p \rangle \approx v_0^p \left( \frac{l}{l_0} \right)^{\zeta_p}, \quad (15)$$

where,

$$\zeta_p = \frac{p}{3} + (3-D)\left(1 - \frac{p}{3}\right) \quad (16)$$

It is seen that for the Beta-model (Frish) the exponent  $\zeta_p$  is a linear and constant function of order  $p$ . We must keep in mind that for  $p = 6$  the difference in value from the theory K41 is equal to the  $3-D$  dimension.

For  $p = 2$  we find that the second order of the structure function has the exponent  $2/3 + (3-D)/3$ ; therefore, the energy spectrum in the inertial range satisfies

$$E(k) \propto k^{-\left(\frac{5}{3} + \frac{3-D}{3}\right)} \quad (17)$$

This spectrum is more abrupt than that one of the Kolmogorov-Obukhov  $k^{-5/3}$ . For  $p = 3$ , we obtain  $\zeta_3 = 1$ , as required by the law four fifths of Kolmogorov.

The viscous cut point for the Beta-model is obtained by equating of the Foucault rotation time  $tl$  to the viscous diffusion time. This gives the following dissipation scale as shown by Frish:

$$\eta \approx l_0 R^{-\frac{3}{1+D}} \approx l_0 R^{-\frac{1}{1+h}} \quad (18)$$

From the multifractal point of view, we proceed to derive the expression for the structure function of order  $p$ .

$$\frac{S_p(l)}{v_0^p} \equiv \frac{\langle \delta v_l^p \rangle}{v_0^p} \approx \int d\mu(h) \left( \frac{l}{l_0} \right)^{ph+3-D(h)} \quad (19)$$

Having fractal dimension as a function of the traffic intensity  $i$ , we can thereby define the fractal dimension  $D(i)$  also as a function of the image scale. This dimension is usually calculated in following way:

$$D(i) = -\text{Log}(N(i)) / \text{Log}(l, i), \quad (20)$$

where,  $N(i)$  is the number of boxes of size  $l$  necessary to cover the image contour of intensity  $i$ . The algorithm used by ImaCalc program operates by dividing the 2D surface into consequent set of small square boxes and by counting the number of boxes which have scales close to the level under study during a number of iterations  $n$ . For each box of size  $l/n$  it is then found if the convoluted line is intersecting that box. Finally, the slope of  $N$  versus the size of the box  $l$  in a log-log plot within experimental limits gives the fractal dimension for a single intensity. Limits of scales in the vicinity of 0 can be measured by counting the number  $N$  of boxes necessary to cover the boundary of the vortices structure generated by the wind turbine. This aspect is also important for decreasing effect of the wake energy investigation.

There are several methods for implementing multifractal analysis; the moment method uses mainly three functions: This method of box-counting in ImaCalc software is used to detect the self-similar

behavior. This analysis can be made for the Scalar marker, for a vector, such as a Vorticity, or a generalized variable. In a mono-fractal object, the number  $N$  of features of a certain size  $e$  varies as

$$N(l) = c(l, i) \exp \{-D_0 l\}, \quad (21)$$

where  $D_0$  is the fractal dimension at the limit of small size exponent function  $\tau(q)$  the coarse Holden exponent,  $\alpha$  and the multifractal spectrum,  $f(\alpha)$  as seen in figure 11. We have only used a grey tone between 0 to 255, in our examples.

## 4 Problem Statement of Wind Turbine Interactions

Studying of wind turbine performance is very effective instrument during manufacturing since it allows improving of the future turbine efficiency on the earlier stages. Furthermore, is important to study the turbulence aspect to estimate an effective separation distance between two turbines and to understand how the wake from one turbine affects the other ones. Investigation of the interaction between the single wake turbine or turbines array and the Atmospheric Boundary Layer can reveal aspects of direct and inverse cascades within the complex flows. Moreover, resonance phenomena are basically assumed to take place when non-homogeneity and intermittency takes place.

### 4.1 Experimental tests

The experiments under consideration were carried out in the Norwegian University of Science and Technology NTNU (Trondheim, Norway) and in the EnFlo Laboratory of University of Surrey (Guildford, UK). In this section we discuss the experiments and numerical results of different combination of wind turbines in the wind channel.

#### 4.1.1 Single wind turbine

Our first goal was to study the turbulence of the turbine wake, of its vortex structure and of the energy dissipation along the wake using the fractal dimension as well as to analyze wake evolution along the time and its interaction with the Atmosphere. We have studied a single turbine with 3 blades which is the most typical design in the world as shown in figure 1. The radius of blade was 63.0 meters, the turbine hub radius was 1.5 meters, the tower height was 87.6 meters, the rotor speed was 9.15 rpm. The resulting flow fields of the wake generate by the turbine are presented below (figure 2)

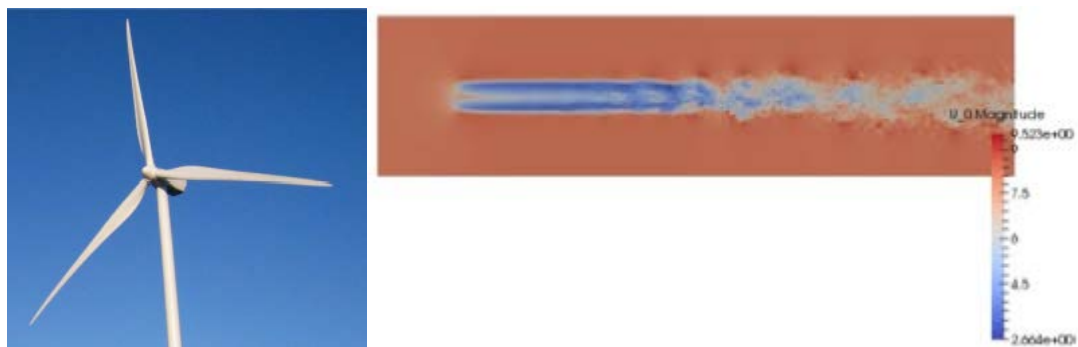


Figure 1: Velocity magnitude of the wake turbine of three blades

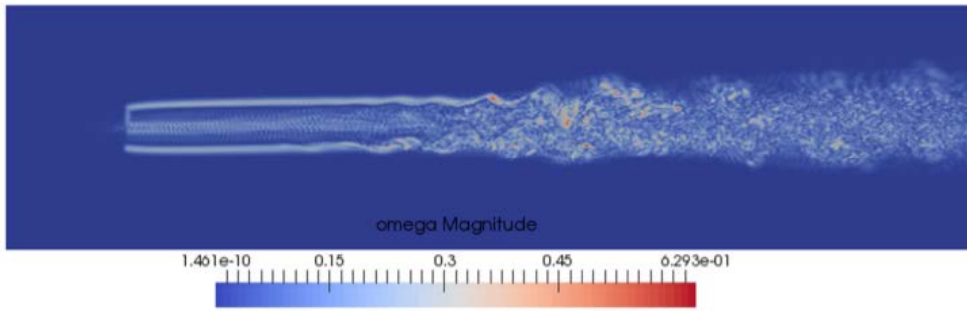


Figure 2: Vorticity structure of the wake

This first study was devoted to methodology testing. The test is described more extensively in [15], where numerical results were used to calculate the maximum value of fractal dimension selected among all of the velocity and vorticity intensities and to obtain the evolution of turbulence spectra in the wake.

#### 4.1.2 Two wind turbine test

In the next test with two wind turbines they were defined the same way as a number of profiles with a tabulated aerodynamics data. Filtered Navier-Stokes equations were solved by LES. The simulation was dedicated to numerical modeling of Blind Test 4 experiment where 2 model wind turbines were presented in wind tunnel (figure3) at average reference speed of  $U_{ref}=11.5$  m/s and at Reynolds number  $Re=100.000$  [16,17].

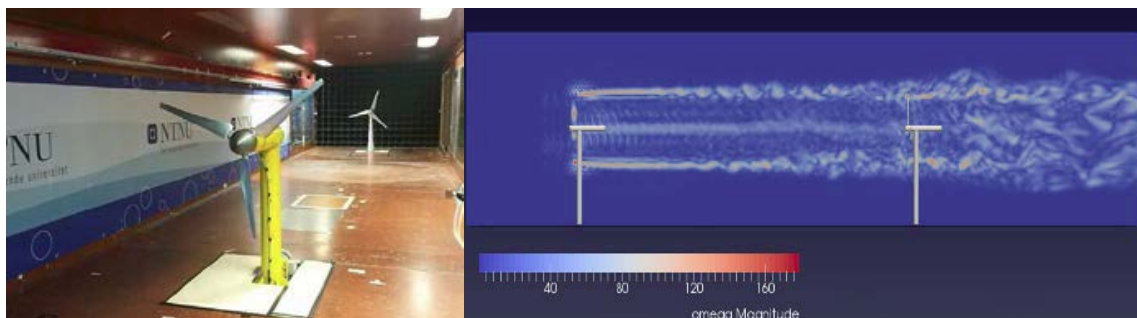


Figure 3: 2 wind turbine in wind tunnel and vorticity structure at  $t=2$ second.

The results of velocity field prediction, profile of velocity normalized by  $U_{ref}$  were improved by introducing the tower and the hub geometry to the model. The comparing of resulting numerical and experimental velocity profiles, generated power  $C_p$  and axial loads  $C_T$  factors, and also the multifractal spectrum  $f(\alpha)$  of the flow were cited in paper [18].

#### 4.1.3 Twelve wind turbine test

The next stage was to study a model test with 12 wind turbines carried out in wind tunnel of University of Surrey (figure 4). A 3-wide 4-deep array of wind turbines was subjected to the external flow with the velocity set to  $U_{ref}=1.5$  m/s [19, 20]. Atmospheric Boundary Layer model was introduced to represent experimental conditions. Parameters of Neutral ABL used in simulation are listed in Table 1. Two different meshes with 4.6 and 8 million cells were used for unsteady simulations. The main results of this paper are based on this last simulation.

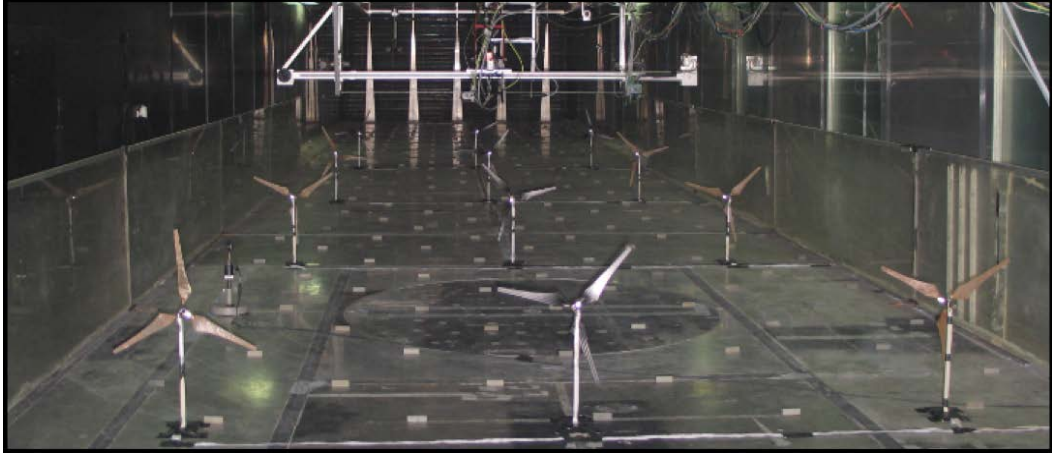


Figure 4: View of wind turbines in the working section, looking upstream.  
A 3-wide  $\times$  4-deep array [20]

Table 1: parameters for the stable, unstable and neutral cases [20]

	<i>Neutral</i>	<i>Stable</i>	<i>Acceleration</i>
$H$ (mm)	$\cong 1050$	$\cong 500$	$\cong 1200$
$k$	0.4	0.4	0.4
$Z_0$ (mm)	$0.10 \pm 0.01$	0.11	0.10
$Z_{0\theta}$	-	0.0004	0.002
$h/L_0$	-	0.4	-1.26
<i>Imposed gradient above</i> $h$ , (k/m)	-	$\cong 20$	$\cong 3$
$\theta_0$ ( $^{\circ}\text{C}$ )	-	16	45
$\left(\frac{(u^2)^{-1}}{U}\right)$ <i>Hub Height (%)</i>	7.3	4.5	9.5

## 5 Results

This section discusses the wake characteristics of 3D domain of the case with 12 wind turbine array. Two unstructured meshes with 4.6 and 8 millions of cells were constructed for the simulation. The meshes were refined near tower and nacelle of wind turbines (figure 5). The numerical technique comprised a preliminary simulation with ABLSolver aimed to define the inlet parameters for the major domain, the second step consisted in numerical simulations using pisoTurbineFoam. The solvers allow distinguishing the mean and turbulent wake flows behind turbines in series and the behavior of the whole 12-turbines array. The flow patterns around four turbines aligned to the axis of symmetry of the array were studied to determine general behavior of the resulting flow. It was noted that the wakes behind the first turbines row are more stable, but with the second turbines row the wake turbulent behavior becomes more pronounced. The results of velocity field in the longitudinal plane of symmetry for the array of wind turbines are shown in figure 6.



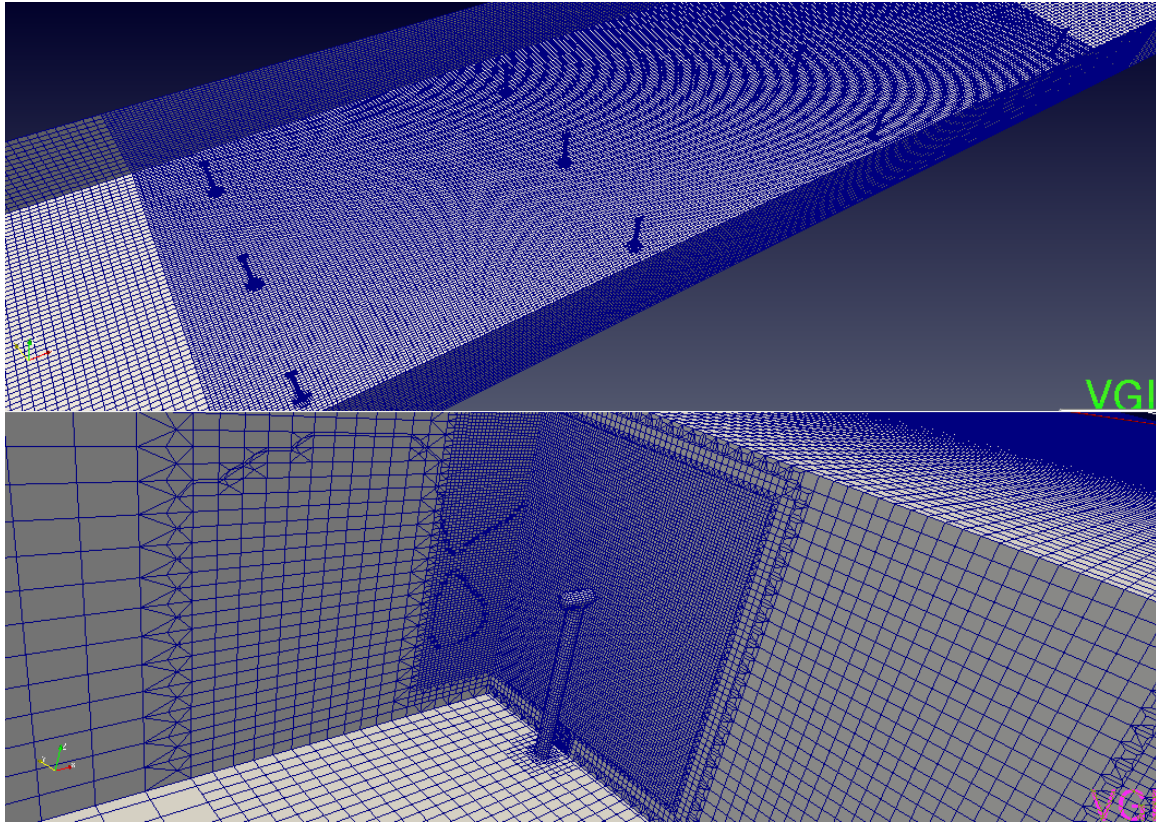


Figure 5: Visualization of numerical domain and refined grid of the wind turbine

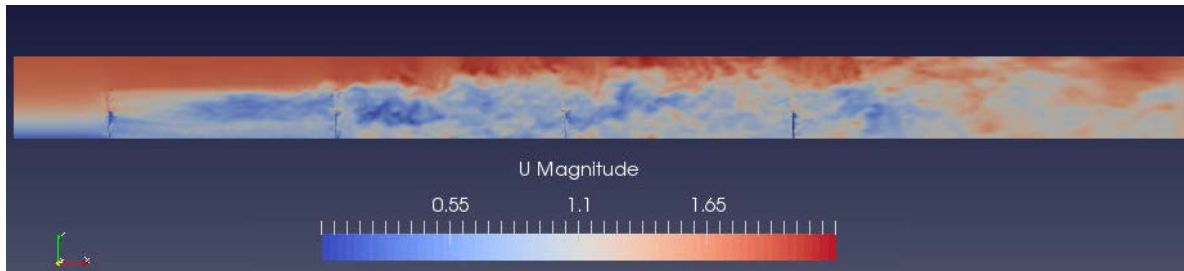


Figure. 6: The velocity field in the longitudinal plane of symmetry of the array for wind turbines (the  $xOz$  plane)

The numerical simulation was carried out in the laboratory of ISP RAS in Moscow, with a computer time elapsed during calculation of the test case (physical time  $t=0.8s$ ) represented in the Table 2:

<i>Number of Processors</i>	<b>Table 2: Computer time of 12 wind turbine</b>		
	<i>Execution time (seconds)</i>	<i>Clock time (seconds)</i>	<i>Acceleration</i>
<i>12 cores in 1 nodes</i>	27573	27650	-
<i>36 cores in 3 nodes</i>	9024	9104	3.04
<i>72 cores in 6 nodes</i>	5399	5842	4.73

In order to study the value of energy spectrum  $E(k)$  with FFTW library a 3D box comprising an even mesh was created. The velocity field was then interpolated into the box and FFT was applied to the filter (figure 7). The calculated energy spectrum  $E(k)$  in Fourier space was closed to Kolmogorov-Obukhov  $k^{-5/3}$  spectrum (figure 8).

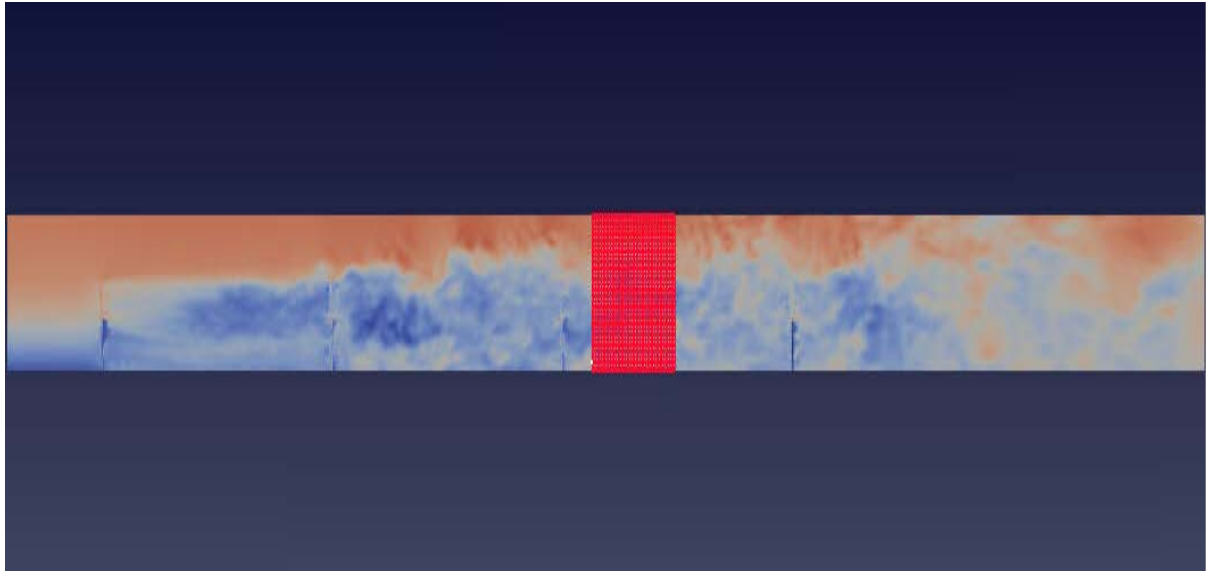


Figure 7: 3D box in numerical domain for calculation  $E(k)$

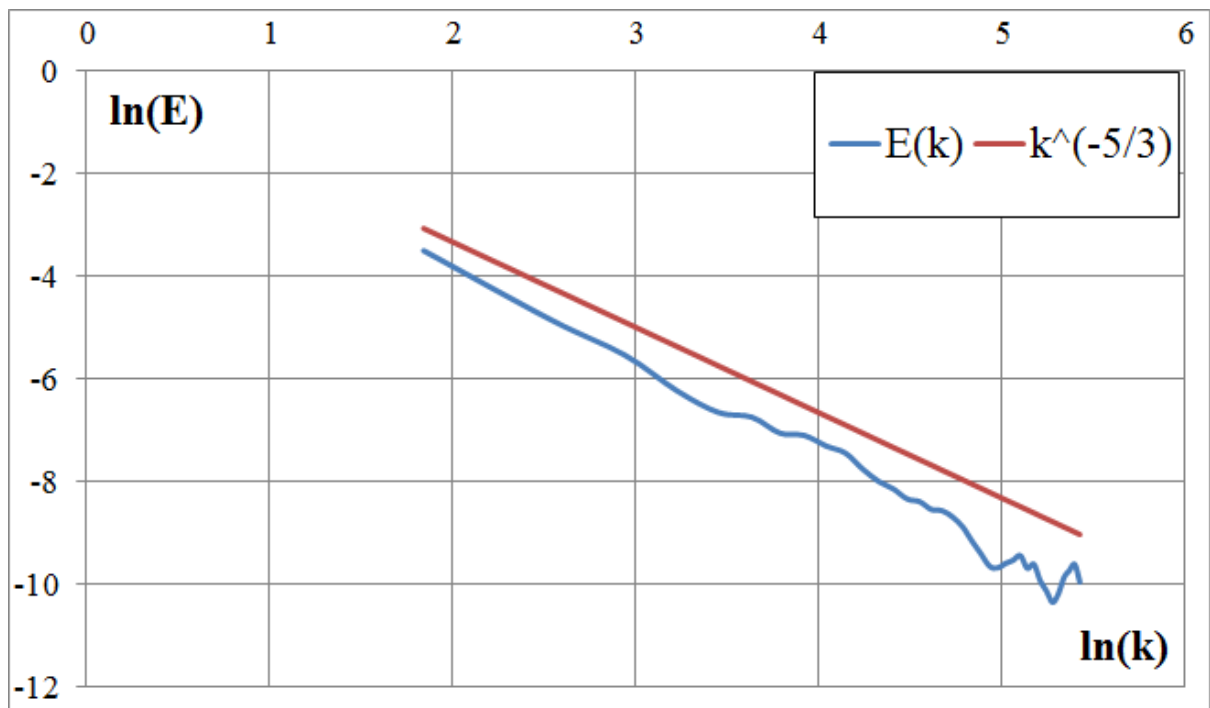


Figure 8: Energy spectrum  $E(k)$

The results of calculation of the horizontal velocity profiles behind the wind turbines are shown in figure 9. The difference with experiment's values of velocity profiles can be explained by using ALM model to simulate flow around wind blades.

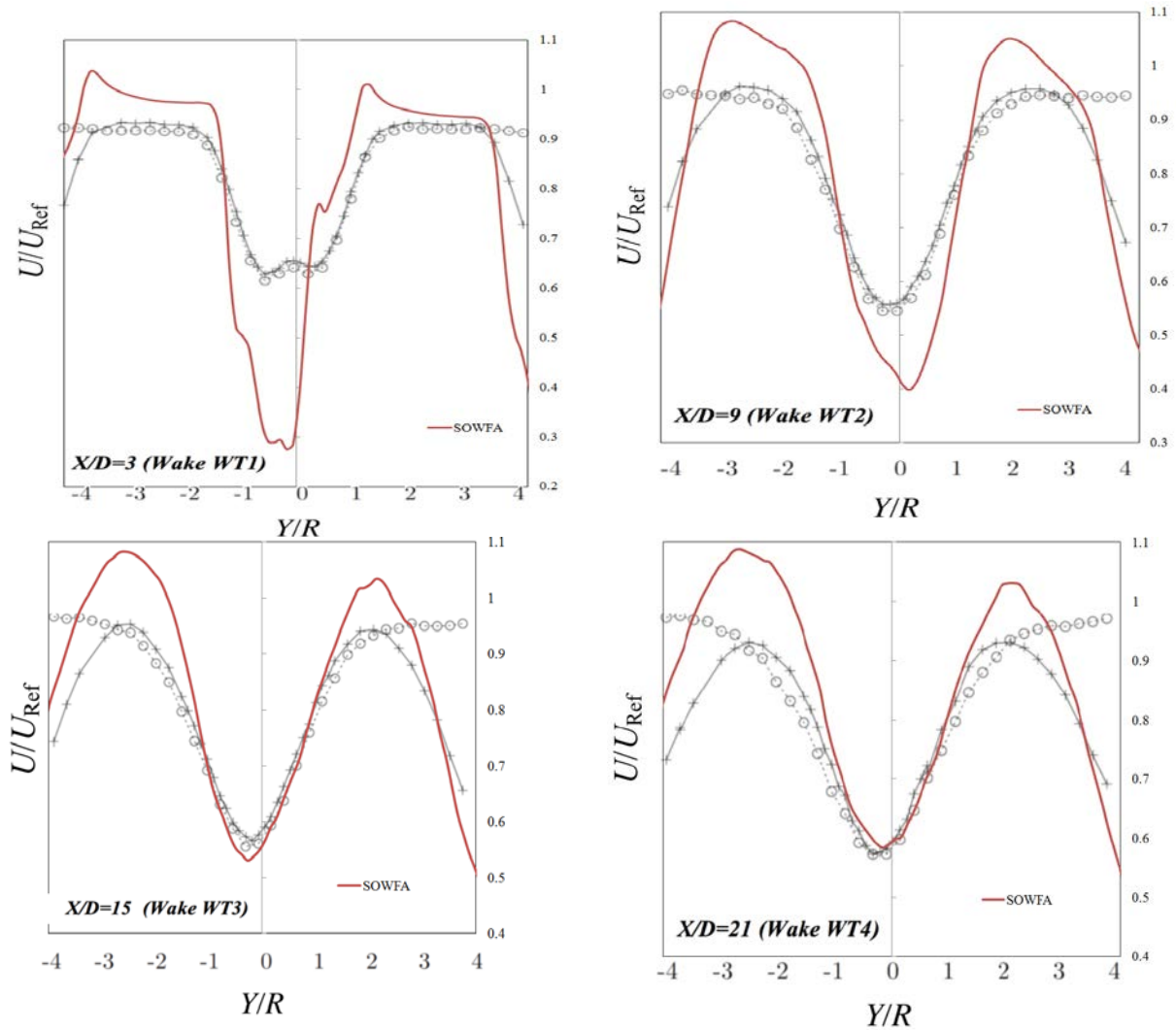


Figure 9: The horizontal velocity profiles behind the wind turbines of the central row in sections  $X / D = \{3; 9; 15; 21\}$ , where  $X$  is the distance from the first wind farm,  $D$  is the diameter of the turbines

## 5.2 Fractal structures in complex wakes of several turbines

The fractal analysis of the turbine wake using the methodology described in section 3 was performed with the help of ImaCalc program. We have calculated the spectrum of the fractal dimension for a set of filter positions taking into account the laminarity of the flow in vicinity of the first turbine and the fact that from the one hand the flow was more non-homogeneous and turbulent starting with the second turbine, but from the other hand the energy decay effect was still presented. Using the fractal method it was possible to study the complexity of wake growth and its interaction with the ABL (figure 10).



Figure 10: Propagation of the wind along the sequence of wind turbines

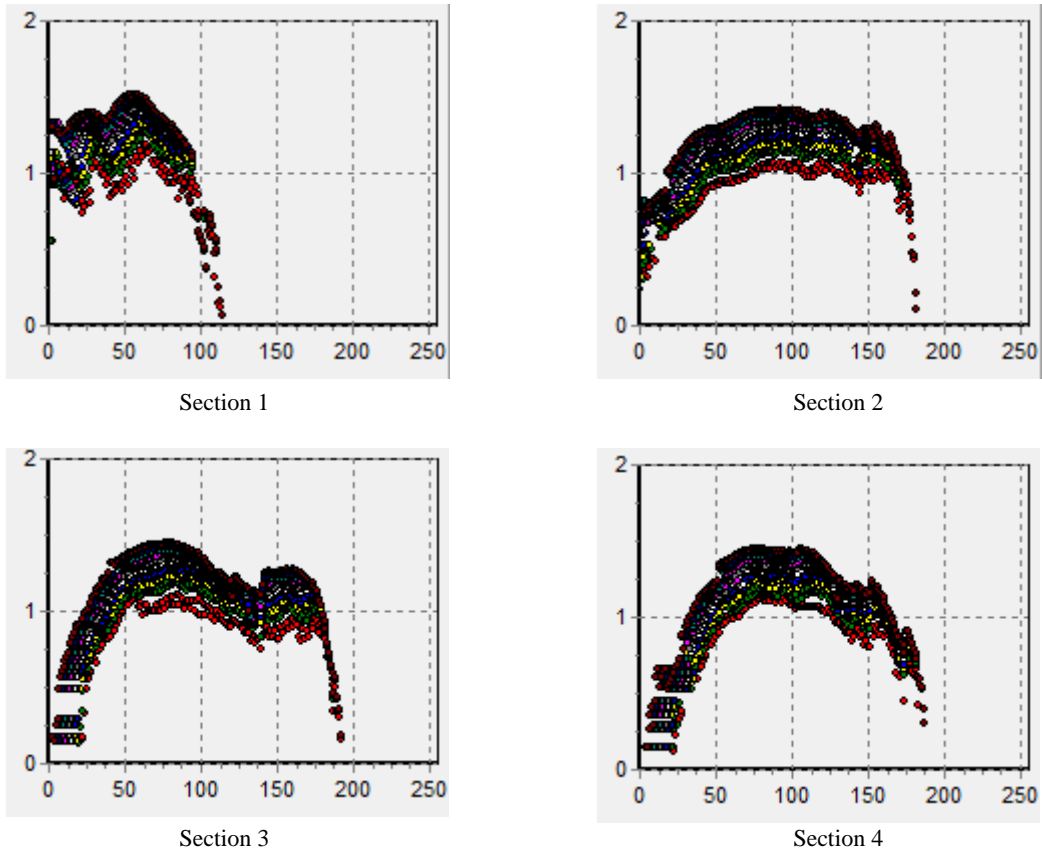


Figure 11: Results of data processing by means of ImaCalc program: the multifractal spectrum  $f(\alpha)$  for the different sections marked in figure 10. Both the range of velocity values (i) and the shape of the multi fractal spectra change in a non/linear fashion.

### 5.3 Diffusion and propagation of the ABL

It is also essential to know the wave propagation effect and the turbulence aspect of the turbine wake. There are several important factors to be considered such as temperature, humidity, wind, type of wind energy, atmospheric pressure, etc. The diffusion along the sequence of wind turbine is possible to study throughout the analysis of structure functions with Fourier transforms, studying the intermittency at different scales. The overall results of the simulation for a set of 12 turbines in wind tunnel contain information on instantaneous and average velocity, pressure, viscosity, energy, stress tensor fields.

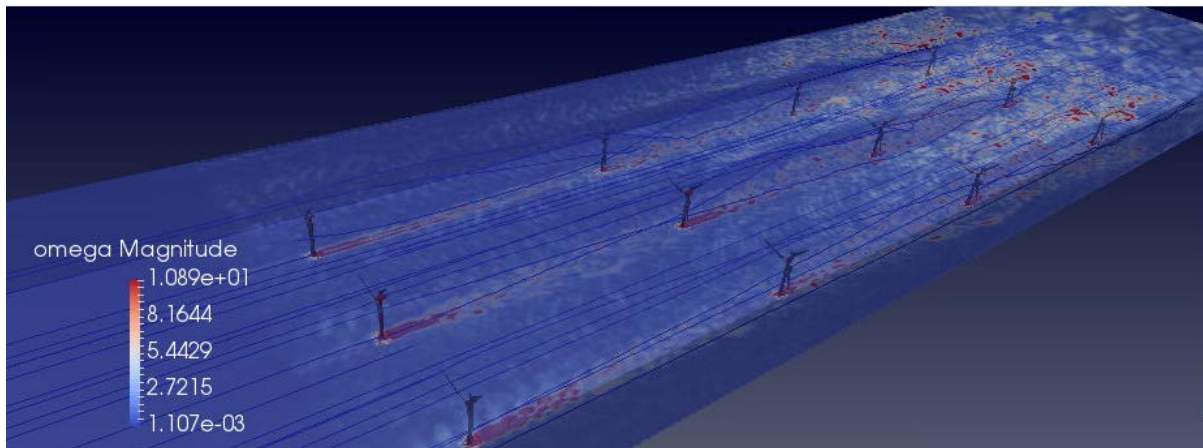


Figure 12: Structure of velocity (time = 20 seconds)

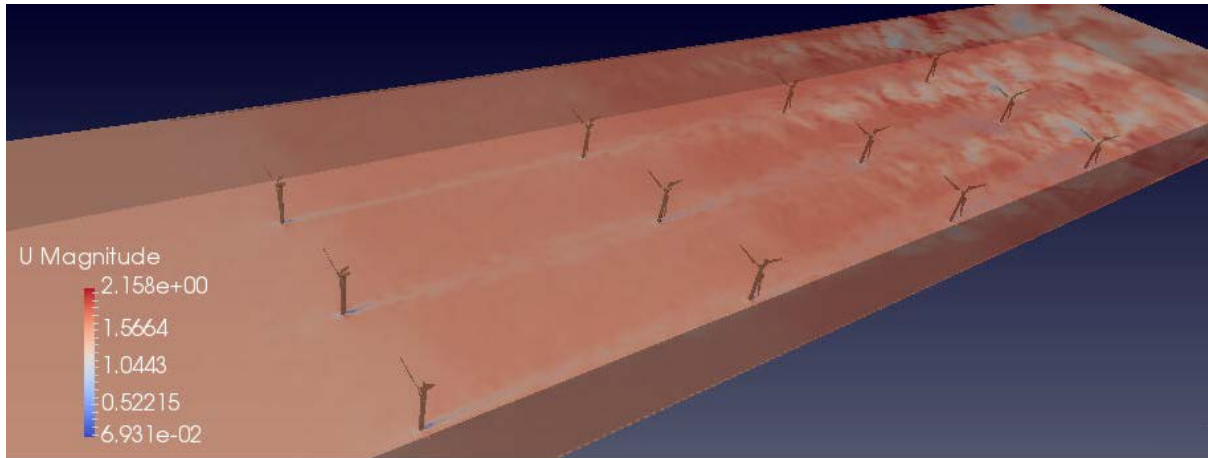


Figure 13: Structure of velocity (time = 20 seconds)

Diffusion and propagation of the waves and vortexes generated by the turbine (figure 13) show the decay energy effect of the flow perturbation. Using qualitative visualization of the wake it is possible to describe the turbulence generation along the set of turbines. It can be noted see that the energy decay is more evident after the second wind turbine, while the Atmospheric Boundary Layer starts to be chaotic or turbulent and the structure of vortexes is much more considerable than behind the first wake. The structure of the ABL behind the last 2 turbines is more similar, comprising coherent structures, or so-called Rayleigh-Taylor bubbles resembling compressible flows or cloud growing due to the cumulative effect of the wind turbines (figure 14).

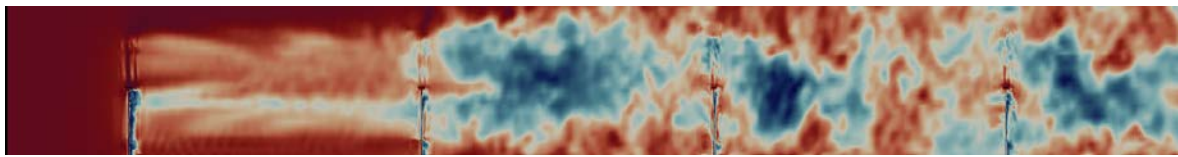


Figure 14: Turbulence behavior of the interaction between wind turbine and ABL, the difference with figure 10, where the downstream sections are marked is that here the additional turbulence produced by the Atmospheric boundary Layer (ABL) is an additional source of intermittency.

The advantage of these complex simulations is to focus on the efficiency of the turbine and of the wind turbine farm. In this study only one angle in a Cartesian system is shown, but many other configurations are possible. Some benefits from the multi-fractal and the structure function analysis originate from the ability to make samples based on the geometry or topology of the scale to scale transfer of momentum, energy or vorticity in the inner structure of the turbulence scaling, e.g., while analyzing only the average velocity integrated in one of the sections. We can see that after the second turbine, the wind velocity decays appreciably, and for this reason the production of energy may be hampered. By this simple analysis it will be also possible to determine the optimal separation distance between two turbines in a real wind farm. One of the usual effects of the decay of overall local energy is that, when internal waves are also apparent, the propagation of these wakes becomes inversely proportional to the efficiency of the wind turbine of a particular row. In contrast, by looking at the fact that higher velocities (i.e. values of  $(i)$  between 130 and 180 in figure 10) drop in complexity,  $D(i)$  between section 2 and section 3 is an indication that an inverse cascade, as well as accumulation of larger resonant structures in that range of velocities and sizes take place. Note that when dominant eddies of the size of the blades occur, an accident may take place.

## 6 Conclusions

The structure of the wind turbines wakes show the complexity of their application due to the effects of rotation and stratification caused by the initial logarithmic wind profiles. The results match qualitatively collected data on similar large scale experiments and numerical calculations. Observation of smoother vorticity contours than the velocity ones provides an opportunity to adequately calculate also the of other important flow parameters scaling (velocity, pressure, vorticity, shear, stress tensor) for a wake behind a single wind turbine. ImaCalc program was used to calculate the value of fractal dimension based on the velocity and vorticity contours. The intermittency exponent changed for higher values of vorticity at an increasing rate from 1.1 for low values up to the maximum of 2.4. The corresponding values of  $H$  varied from 0.2 to 1.5 for different sections. For wakes going through several arrays of turbines, there seems to be a strong inverse cascade, but only for the largest ranges of velocity. It is also detected that the intermittency exponent  $\mu$  changes with the levels of vorticity values for a developed vorticity wake behind a wind turbine. Non-orthogonal arrays of turbines are still in great need of being studied. In some cases, even if the second or third row of turbines diminish the available energy, dangerous resonances due to both generation and cascade intermittency may appear [18, 21].

It is planned further to perform research of nonlinear dynamics of vortex structures in the wakes of more complex and higher Reynolds flows. We have also measured that the third order structure scaling exponent is not exactly equal to 3, it means that intermittency acts as a natural compensating effect on the scale to scale transfer of energy. This possible behavior is believed to take place in other non-homogeneous flows. High order statistics of velocity increments like skewness and flatness at hub height and in tip regions of wind turbine are the key indices of how to improve numerical simulations by using various subgrid-scale models for LES. Comparing measurements and simulations of higher order structure functions can drop light on the mechanism of turbine rotational dynamics changes and resonances in the turbulent wakes caused by intermittency.

The calculations were run using resources of a high-performance cluster with 12-72 cores for each single case, in the scope of UniHUB web-laboratory of ISPRAS.

## Acknowledgements

The project was supported by RFBR (grant No. 17-07-01391). We also thank ERCOFTAC the BSC and the RES for the facilities provided and the PELNoT for travel support.

## References

- [1] R.J.A.M. Stevens, C. Meneveau. Flow Structure and Turbulence in Wind Farms, *Annu. Rev. Fluid Mech.*, 49: 311–39, 2017.
- [2] M.J. Churchfield, S. Lee, J. Michalakes, P.J. Moriarty. A numerical study of the effects of atmospheric and wake turbulence on wind turbine dynamics. *Journal of Turbulence*, vol. 13, 14: 1–32, 2012.
- [3] P. Sagaut. Large eddy simulation for incompressible flows: an introduction. Springer, Berlin. 2002, p. 426.
- [4] C. Meneveau, T.S. Lund, W.H. Cabot. A Lagrangian dynamic subgrid-scale model of turbulence. *J. Fluid. Mech.*, 319: 353–385, 1996.
- [5] J.N. Sørensen, W.Z. Shen. Numerical Modeling of Wind Turbine Wakes, *Journal of Fluids Engineering*, 124: 393-399, 2002.
- [6] L.A. Martínez-Tossas, et al. Large eddy simulations of the flow past wind turbines: actuator line

- and disk modeling. *Wind Energy.*, vol.18, 6: 1047-1060, 2014.
- [7] S. B. Pope, *Turbulent Flows*. Cambridge University Press, 2000.
- [8] J.C. Vassilicos. *Intermittency in Turbulent Flows*. Cambridge University Press. 2001.
- [9] U. Frisch, P.-L. Sulem, M. Nelkin. A simple dynamic model of intermittent fully developed turbulence. *J. Fluid Mech.*, 87: 719-736, 1978.
- [10] O. Ben-Mahjoub, A. Babiano and J.M. Redondo. Velocity structure and Extended Self Similarity in non-homogeneous Turbulent. *Jets and Wakes*. *Applied Scientific Research*. 59: 299-313. 1998.
- [11] J.M. Vindel, C. Yage, J.M. Redondo. Structure function analysis and intermittency in the atmospheric boundary layer. *Nonlinear Processes Geophys.*, 15: 915-929, 2008.
- [12] R. Stresing, J. Peinke, R.E. Seoud, J.C. Vassilicos. Defining a New Class of Turbulent Flows. *Physical Review Letters*, vol. 104, 194501: 1-4, 2010.
- [13] J. M. Redondo, J. Tellez, J. Kopeck, K. Kwiatkowski, P. Lopez, M. Tijera, S. Strijhak, N. Malik, O. B. Mahjoub, S. Usama: Fractal Intermittent Wakes in a Wind Tunnel. In *Proceedings Topical Problems of Fluid Mechanics 2018*, Prague, 2018 Edited by David Šimurda and Tomáš Bodnár, 243-250, 2018.
- [14] N. Ali, et al. Structure functions, scaling exponents and intermittency in the wake of a wind turbine array. *Journal of renewable and sustainable energy*, 8: 013304-1 - 013304-9, 2016.
- [15] S. Strijhak, J.M. Redondo, J. Tellez. Multifractal Analysis of a Wake for a Single Wind Turbine. In *Proceedings Topical Problems of Fluid Mechanics 2017*, Prague, 2017 Edited by David Šimurda and Tomáš Bodnár, 275-284, 2017.
- [16] F. Pierella, P. Å. Krogstad, L. Sætran. Blind Test 2 calculations for two in-line model wind turbines where the downstream turbine operates at various rotational speeds,” *Renew. Energ.*, 70: 62–77, 2014.
- [17] J. Bartl, L. Sætran. Blind test comparison of the performance and wake flow between two in-line wind turbines exposed to different turbulent inflow conditions, *Wind Energ. Sci.*, 2: 55–76, 2017.
- [18] A. Kryuchkova, J. Tellez-Alvarez, S. Strijhak, J.M. Redondo. Assessment of turbulent wake behind two wind turbines using multi-fractal analysis. *Ivannikov ISPRAS Open Conference (ISPRAS)*, 110-116, 2017.
- [19] P. E. Hancock, F. Pascheke. Wind-Tunnel Simulation of the Wake of a Large Wind Turbine in a Stable Boundary Layer: Part 2, the Wake Flow. *Boundary-Layer Meteorol*, 151:23–37, 2014.
- [20] P.E. Hancock P.E., T.D. Farr. Wind-tunnel simulations of wind-turbine arrays in neutral and non-neutral winds. *J. Phys.: Conf. Ser.* 524 012166, 2014.
- [21] Strijhak S. and Kalugin M.D , Analysis of the vortex structure dynamics in the ABL using LES and POD. *Ercoftac Bulletin*, 114, 12-16, 2018.